

1. P 23 p. u

X62-11095

Copy

54

NASA TM X-730

NASA TM X-730

162-11104 2

(NASA-TM-X-730) STATIC LONGITUDINAL
AERODYNAMIC CHARACTERISTICS OF A 0.028
SCALE MODEL OF A PROPOSED LITTLE JOE-APOLLO
SPACE VEHICLE AT MACH NUMBERS FROM 1.50 TO
2.16 R.H. Fournier (NASA) Oct. 1962 23 p 00/99 N72-73000
Unclas 30871

TECHNICAL MEMORANDUM

X-730

STATIC LONGITUDINAL AERODYNAMIC CHARACTERISTICS OF A
0.028-SCALE MODEL OF A PROPOSED LITTLE JOE-APOLLO SPACE
VEHICLE AT MACH NUMBERS FROM 1.50 TO 2.16

By Roger H. Fournier
Langley Research Center
Langley Station, Hampton, Va.

CLASSIFICATION MARKED
UNCLASSIFIED
By Authority of 1272207 Date 5/15/72

CLASSIFIED DOCUMENT - TITLE UNCLASSIFIED
This material contains information affecting the national defense of the United States within the meaning of the espionage laws, Title 18, U.S.C., Sec. 793 and 794, and the transmission or revelation of information in any manner to an unauthorized person is prohibited by law.

NATIONAL AERONAUTICS AND SPACE ADMINISTRATION
WASHINGTON
October 1962

launching of the full-scale vehicle, test the egress system proposed for the Apollo spacecraft. Longitudinal aerodynamic characteristics of the model were determined at Mach numbers from 1.50 to 2.16, at angles of attack from about -5° to 18° , and at a Reynolds number of 3.5×10^6 per foot. The model was tested with and without stabilizing fins located at the model base of the Little Joe launch vehicle. Although the model was statically stable throughout the angle-of-attack and Mach number ranges covered in the present investigation, transonic results for this model (ref. 1) indicated static instability for a typical center-of-gravity location at all subsonic Mach numbers of the investigation.

COEFFICIENTS AND SYMBOLS

The data of this investigation are presented about the system of axes shown in figure 1. Moment coefficients are referred to a point located on the model center line 7.250 inches forward of the base of the model and is considered to be a typical center-of-gravity location for supersonic speeds.

A	maximum cross-sectional area of model, 0.1104 sq ft
A_b	area on which base pressure acts, 0.0276 sq ft
C_A	axial-force coefficient, $\frac{\text{Axial force}}{qA}$
$C_{A,b}$	base-axial-force coefficient, $\frac{(p - p_b)A_b}{qA}$
$C_{A_{\alpha=0}}$	axial-force coefficient at $\alpha = 0^\circ$
C_D	drag coefficient, $\frac{\text{Drag}}{qA}$
C_L	lift coefficient, $\frac{\text{Lift}}{qA}$
C_m	pitching-moment coefficient, $\frac{\text{Pitching moment}}{qAd}$
C_{m_α}	slope of pitching-moment curve at $\alpha = 0^\circ$, per deg
C_N	normal-force coefficient, $\frac{\text{Normal force}}{qA}$
C_{N_α}	slope of normal-force curve at $\alpha = 0^\circ$, per deg

NATIONAL AERONAUTICS AND SPACE ADMINISTRATION

TECHNICAL MEMORANDUM X-730

STATIC LONGITUDINAL AERODYNAMIC CHARACTERISTICS OF A
0.028-SCALE MODEL OF A PROPOSED LITTLE JOE-APOLLO SPACE
VEHICLE AT MACH NUMBERS FROM 1.50 TO 2.16*

By Roger H. Fournier

SUMMARY

An investigation has been conducted in the Langley Unitary Plan wind tunnel to determine the static longitudinal aerodynamic characteristics of a proposed 0.028-scale model of a Little Joe-Apollo space vehicle. The effect of stabilizing fins, located at the model base, was determined. The model of the spacecraft had a half-cone angle of 33° , a four-legged tower supporting the abort rocket, and a conic fairing covering the abort-rocket nozzles. The investigation was conducted over a Mach number range from 1.50 to 2.16, an angle-of-attack range from about -5° to 18° , and at a Reynolds number of 3.55×10^6 per foot.

The results of wind-tunnel tests indicate that the fins stabilized the space vehicle throughout the test angle-of-attack and Mach number ranges. The center of pressure, measured from the base, for the model without stabilizing fins was about 0.83 model diameters ahead of the model moment center and for the configuration with stabilizing fins varied with increasing Mach number from 0.48 to 0.27 model diameters aft of the model moment center.

INTRODUCTION

The National Aeronautics and Space Administration has initiated wind-tunnel investigations to determine the static longitudinal aerodynamic characteristics of models of proposed Apollo spacecraft. (See refs. 1 to 4.) As part of this program, tests were conducted at supersonic speeds in the Langley Unitary Plan wind tunnel on a 0.028-scale model of the proposed Apollo spacecraft in combination with the Little Joe launch vehicle. The Little Joe-Apollo combination will, in the

*Title, Unclassified.

d	maximum diameter, 4.500 in.
L/D	lift-drag ratio, C_L/C_D
M	free-stream Mach number
p	free-stream static pressure, lb/sq ft
p_b	measured base pressure, lb/sq ft
p_t	free-stream stagnation pressure, lb/sq in.
q	free-stream dynamic pressure, $0.7\rho M^2$, lb/sq ft
R	Reynolds number
r	radius, in.
T_t	stagnation temperature, °F
X_s, Z_s	stability axes
X,Y,Z	model axes
x_{cp}/d	location of center of pressure measured in model body diameters from moment center (positive values are upstream of moment center)
α	angle of attack of model center line, deg

MODEL AND APPARATUS

Details of the 0.028-scale model investigated are shown in figure 2 and a photograph is presented in figure 3. The model investigated consisted of the Little Joe-Apollo configuration, tested with and without the stabilizing fins located at the base of the Little Joe launch vehicle. The abort system on the Apollo spacecraft model consisted of the escape rocket mounted on the spacecraft by four tower rods which were oriented so that the base of the square formed by the rods was in a horizontal plane. (See fig. 2.) The Apollo spacecraft incorporated the same modifications reported in reference 3; that is, a 33° half-cone angle on the spacecraft and a conical fairing around the abort rocket nozzles.

The tests were conducted in the low Mach number test section of the Unitary Plan wind tunnel. This tunnel is a variable-pressure,

continuous return-flow type with a test section 4 feet square and approximately 7 feet in length. An asymmetric sliding block nozzle provides a means to vary the Mach number continuously from 1.50 to 2.87.

Forces and moments acting on the model were measured by an internally mounted strain-gage balance. The model support system consisted of a balance-model-sting combination attached to a remotely operated adjustable-angle coupling connected to the tunnel central support system. Pressure measurements at the base of the model were made with a pressure-sensitive electrical pickup.

TESTS

The Apollo spacecraft in combination with the Little Joe launch vehicle was tested through a Mach number range from 1.50 to 2.16 and an angle-of-attack range from about -5° to 18° . The model was tested with and without stabilizing fins located on the base of the Little Joe launch vehicle. Test conditions are summarized in the following table:

M	p_t , lb/sq in.	q , lb/sq ft	T_t , $^{\circ}\text{F}$	R/ft
1.50	13.0	803	125	3.57×10^6
1.57	13.1	800	125	3.53
1.80	14.2	807	125	3.55
2.16	16.6	776	125	3.55

CORRECTIONS AND ACCURACY

All angles of attack have been corrected for flow angularity and structural deflection of the sting-balance combination due to the aerodynamic loads. The axial-force and drag coefficients presented are the total values of the forces measured by the balance and have not been adjusted in any way for the pressure acting at the base of the model. The maximum deviation of the local Mach number in the region of the tunnel occupied by the model is ± 0.015 . The estimated accuracies of the angles of attack and the coefficients, based on the balance calibration and the repeatability of the data, are within the following limits:

α , deg	± 0.10
C_N	± 0.017
C_m	± 0.010
C_A	± 0.006
C_L	± 0.006

RESULTS

Typical schlieren photographs for the angle-of-attack range of the investigation at Mach numbers of 1.50 and 2.16 are shown in figure 4. The flow patterns are noted to change significantly with increasing Mach number.

The base-axial-force coefficients are presented in figure 5. Addition of the stabilizing fins shows a slight increase in base-axial-force coefficient, but the effect of Mach number and angle of attack is negligible.

The longitudinal aerodynamic characteristics shown in figure 6 indicate that the addition of the stabilizing fins causes the model to become stable throughout the test Mach number and angle-of-attack ranges. This addition of fins also increases the values of L/D , C_D , and C_N .

The summary of the longitudinal aerodynamic characteristics presented in figure 7 shows that without the stabilizing fins the model is unstable throughout the test Mach number and angle-of-attack ranges but that addition of the fins stabilized the model. The center of pressure for the model without stabilizing fins is about 0.83 model diameters ahead of the model moment center and for the configuration with stabilizing fins varies from 0.48 to 0.27 model diameters aft of the model moment center.

CONCLUDING REMARKS

The results of wind-tunnel tests of a model of the proposed Little Joe-Apollo space vehicle over a Mach number range from 1.50 to 2.16 indicate that the addition of the stabilizing fins stabilized the space vehicle throughout the test angle-of-attack and Mach number ranges. The center-of-pressure location for the model without stabilizing fins was approximately constant throughout the Mach number range and had a value of about 0.83 model diameters ahead of the moment center. However, for the configuration with stabilizing fins the center-of-pressure location varied with increasing Mach number from 0.48 to 0.27 model diameters aft of the model moment center. The addition of the stabilizing fins also increased the axial-force and normal-force coefficients throughout the Mach number and angle-of-attack ranges of the investigation.

Langley Research Center,
National Aeronautics and Space Administration,
Langley Station, Hampton, Va., July 6, 1962.

REFERENCES

1. Pearson, Albin O.: Static Longitudinal Aerodynamic Characteristics of a 0.028-Scale Model of a Proposed Little Joe-Apollo Space Vehicle. at Mach Numbers From 0.50 to 1.20. NASA TM X-692, 1962.
2. Morgan, James R., and Fournier, Roger H.: Static Longitudinal Aerodynamic Characteristics of a 0.07-Scale Model of a Proposed Apollo Spacecraft at Mach Numbers of 1.57 to 4.65. NASA TM X-603, 1961.
3. Pearson, Albin O.: Wind-Tunnel Investigation of the Static Longitudinal Aerodynamic Characteristics of Models of Reentry and Atmospheric-Abort Configurations of a Proposed Apollo Spacecraft at Mach Numbers From 0.30 to 1.20. NASA TM X-604, 1961.
4. Pearson, Albin O.: Wind-Tunnel Investigation of the Static Longitudinal Aerodynamic Characteristics of a Modified Model of a Proposed Apollo Atmospheric-Abort Configuration of Mach Numbers From 0.30 to 1.20. NASA TM X-686, 1962.

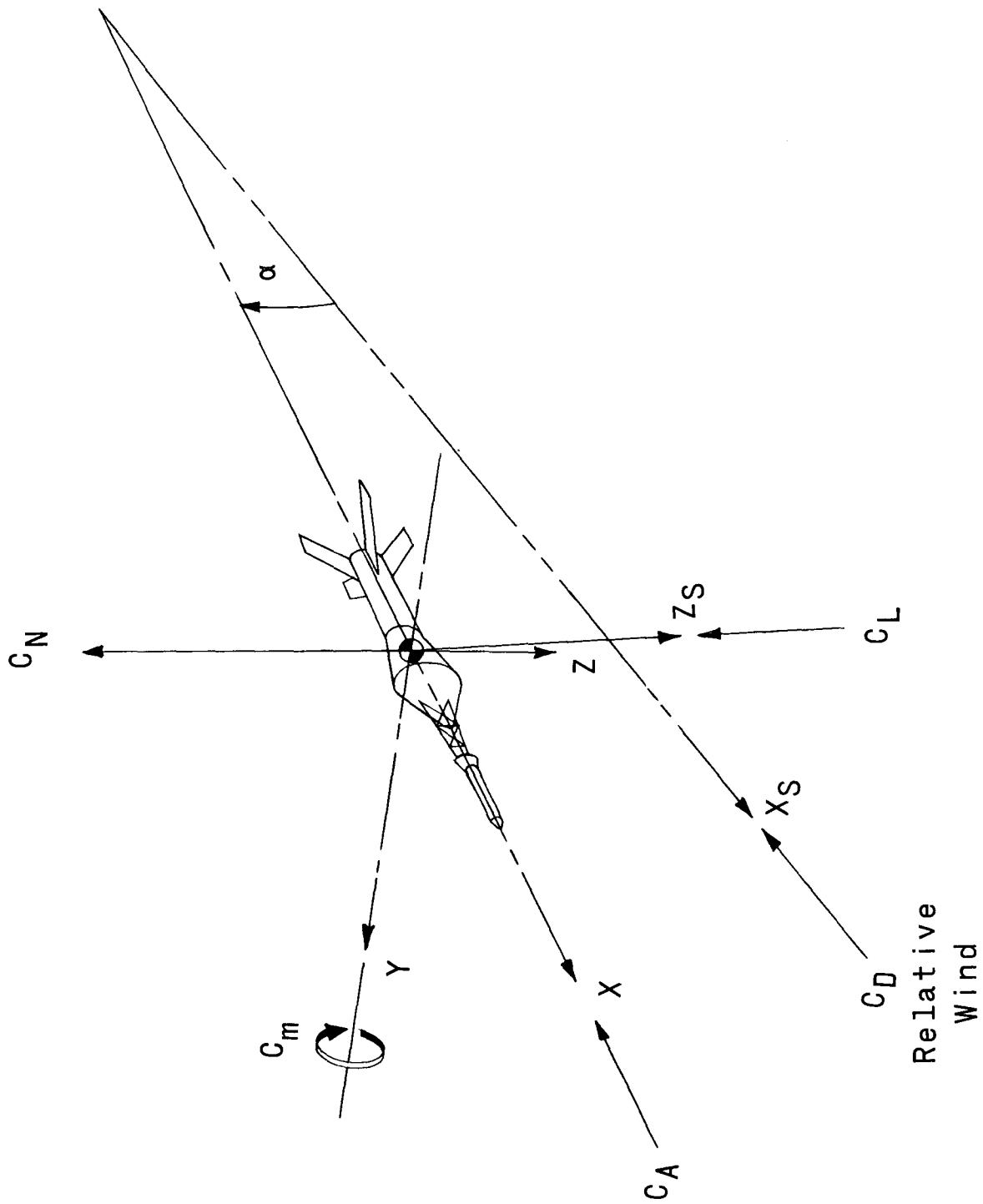


Figure 1.- System of axes. Arrows indicate positive values.

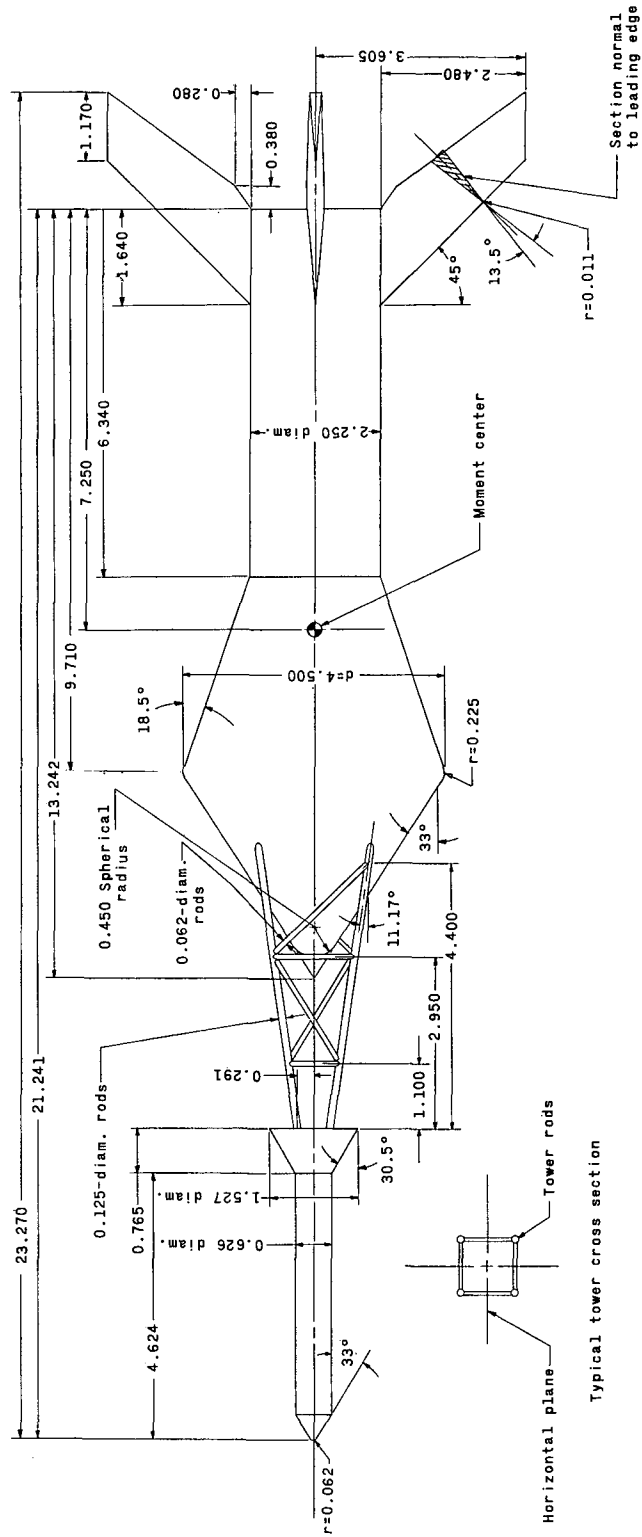


Figure 2.- Details of model tested. All dimensions are in inches unless otherwise noted.

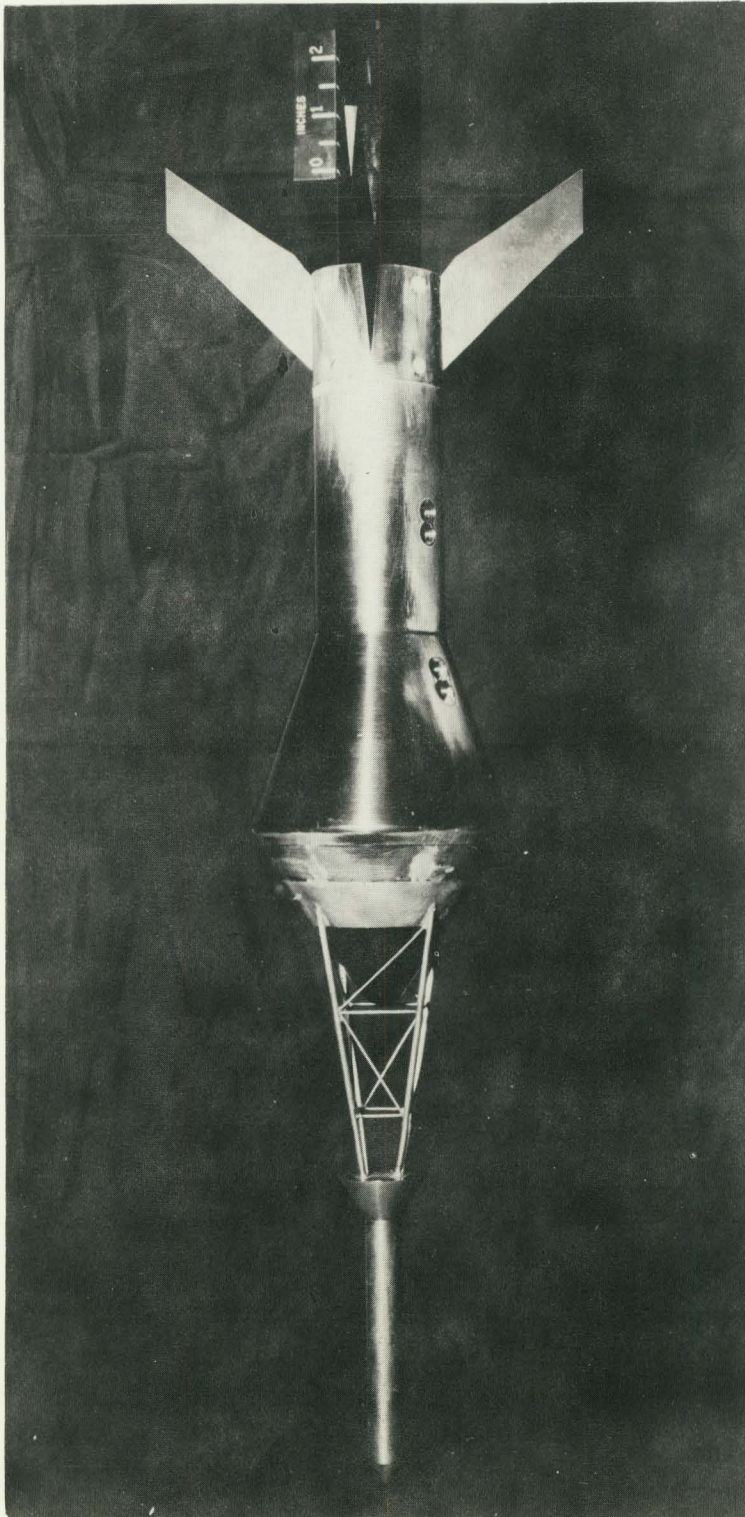


Figure 3.- Photograph of model tested. I-62-2108

CONFIDENTIAL

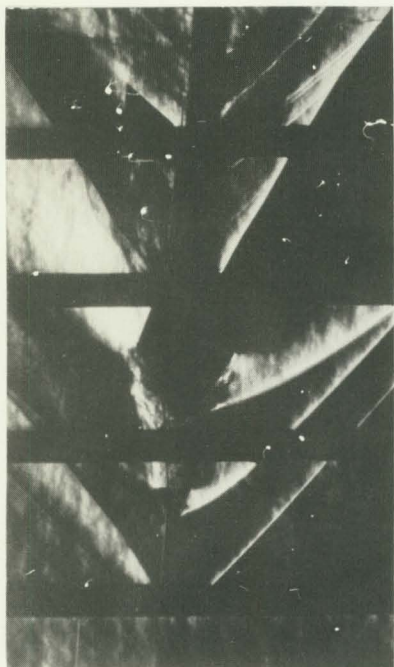
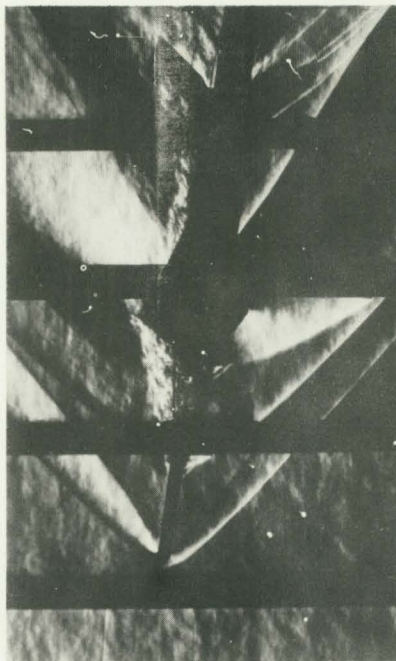
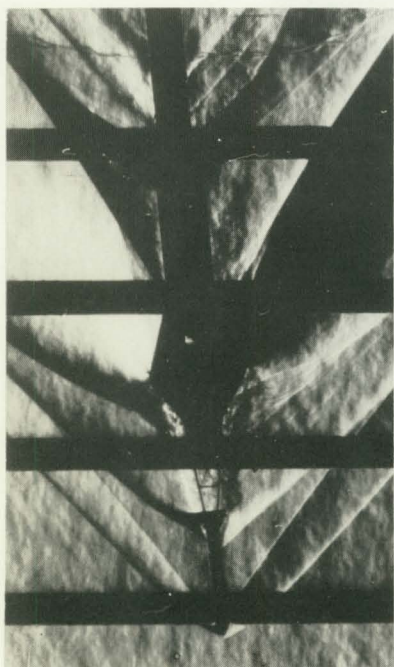
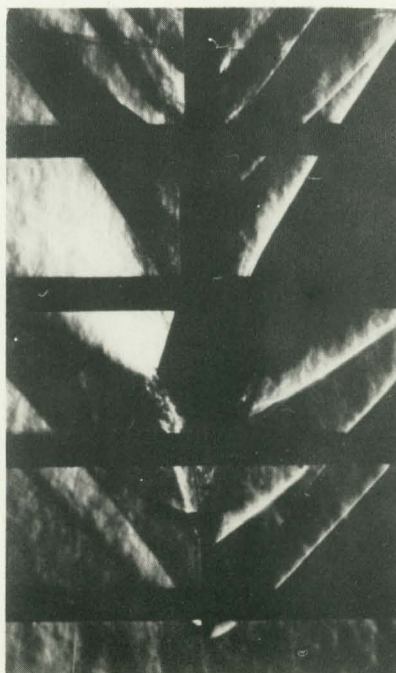
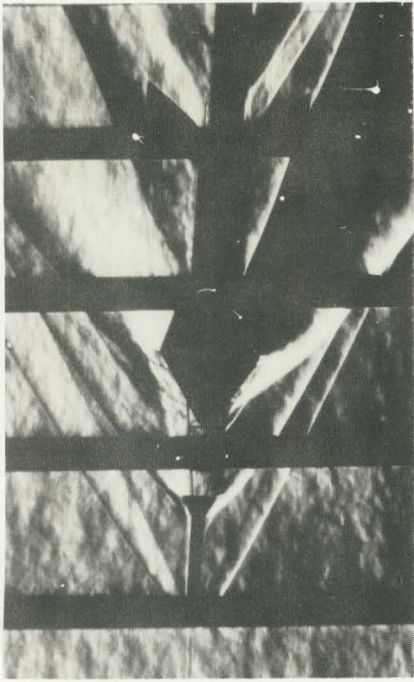
 $\alpha = 5.3$  $\alpha = 9.4$ (a) $M = 1.50$. L-62-2109 $\alpha = 0.2$  $\alpha = 4.8$

Figure 4.- Typical schlieren photographs of model tested.

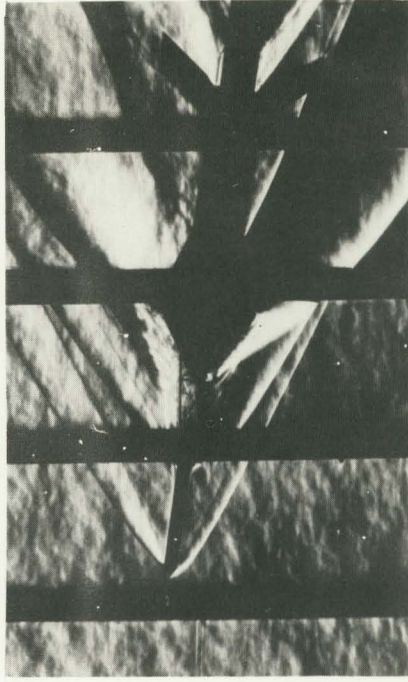
CONFIDENTIAL

CONFIDENTIAL

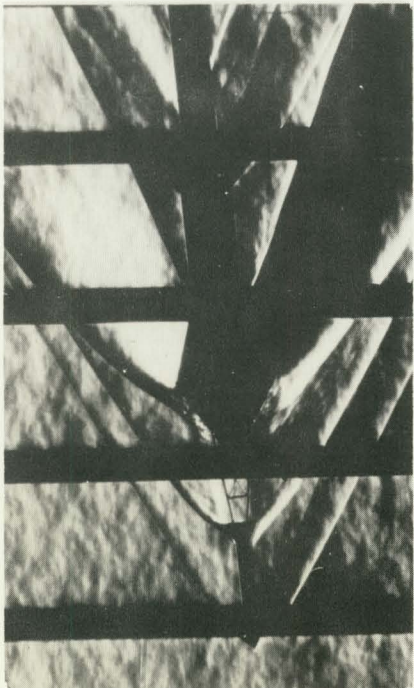
11



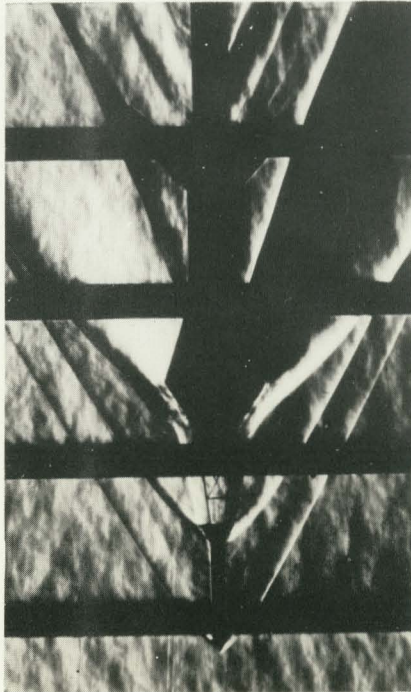
$\alpha = 5.3$



$\alpha = 9.4$



$\alpha = -4.8$



$\alpha = 0.2$

(b) $M = 2.16$. I-62-2110

Figure 4.- Concluded.

CONFIDENTIAL

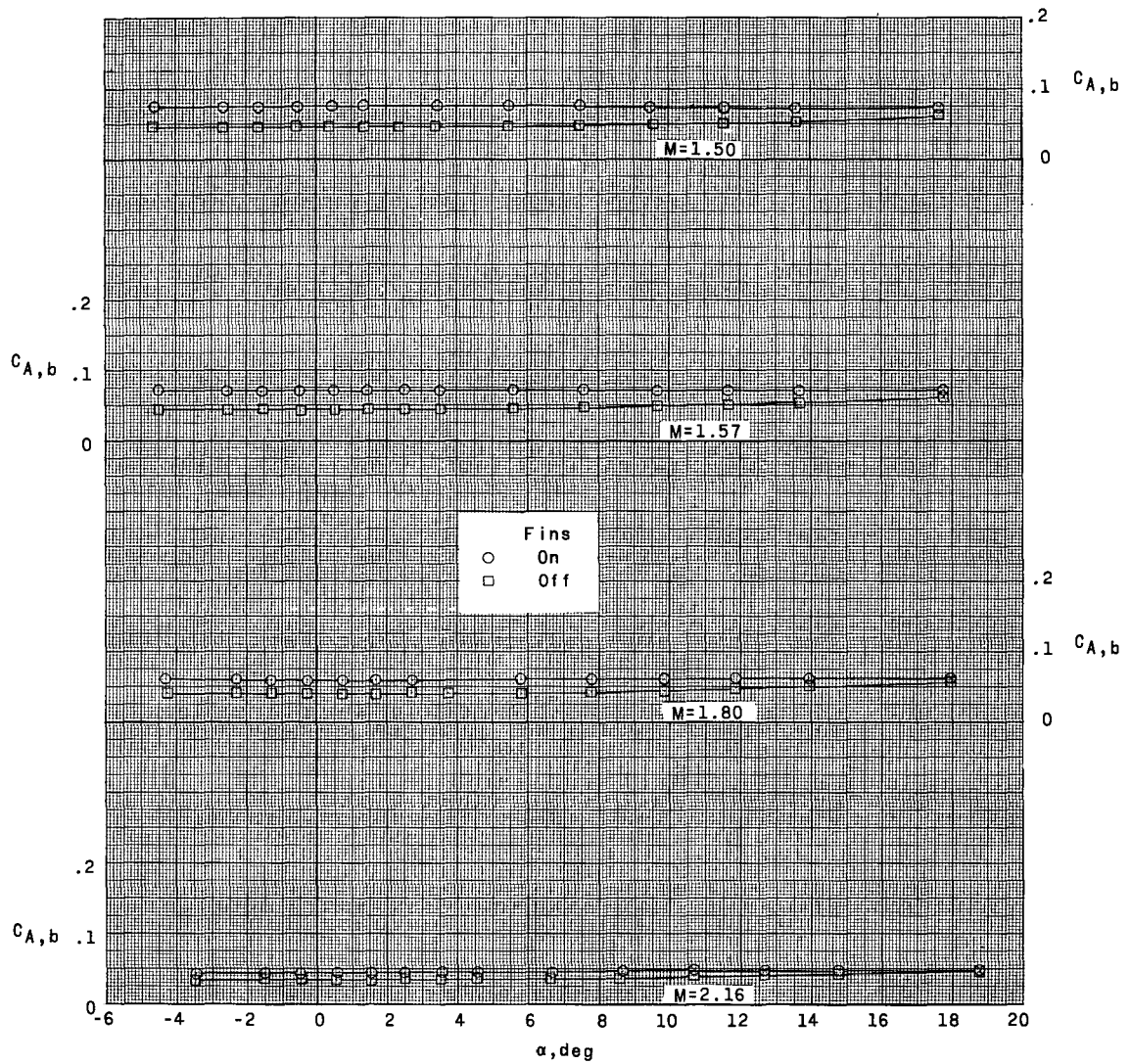


Figure 5.- Base-axial-force coefficient of model.

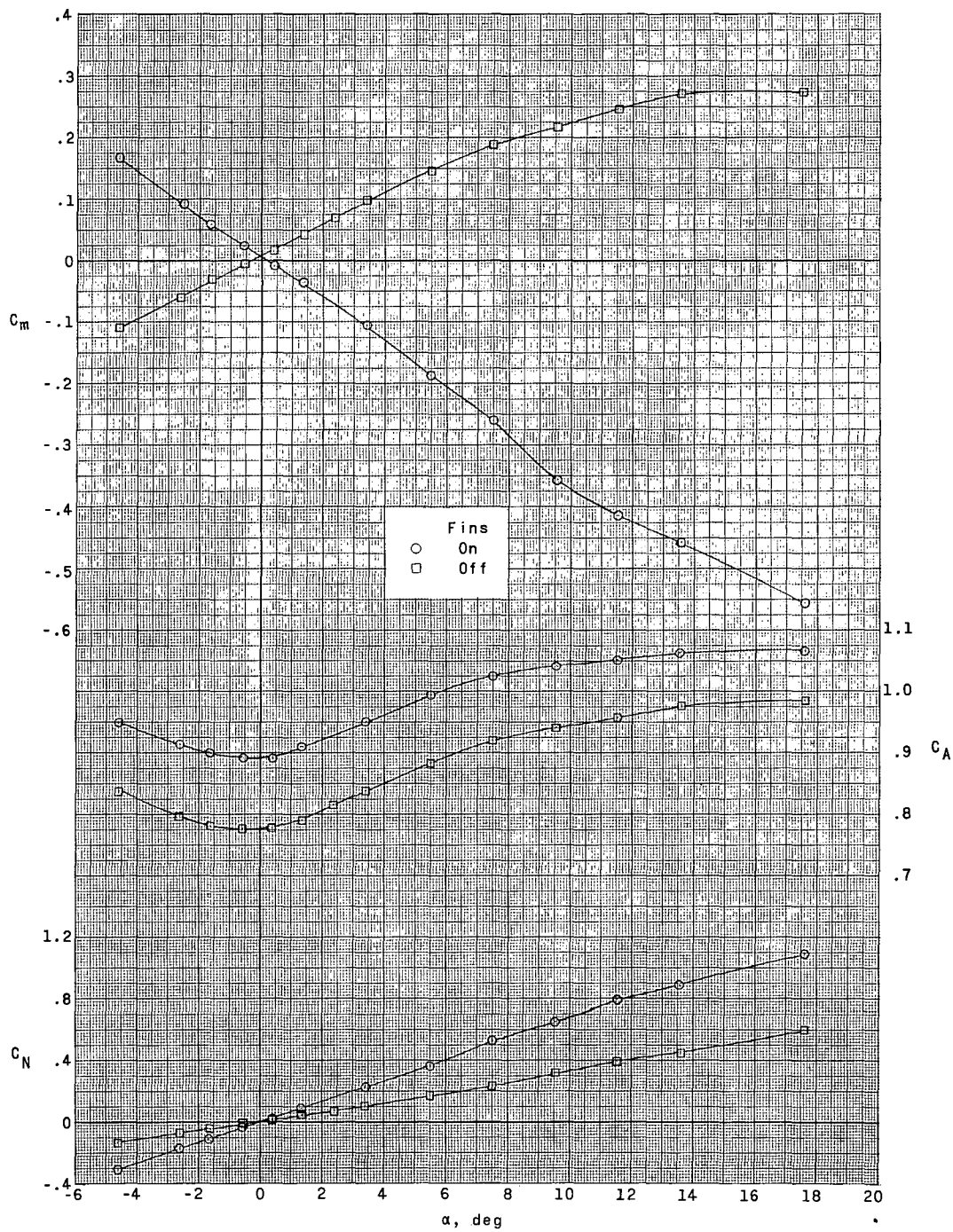
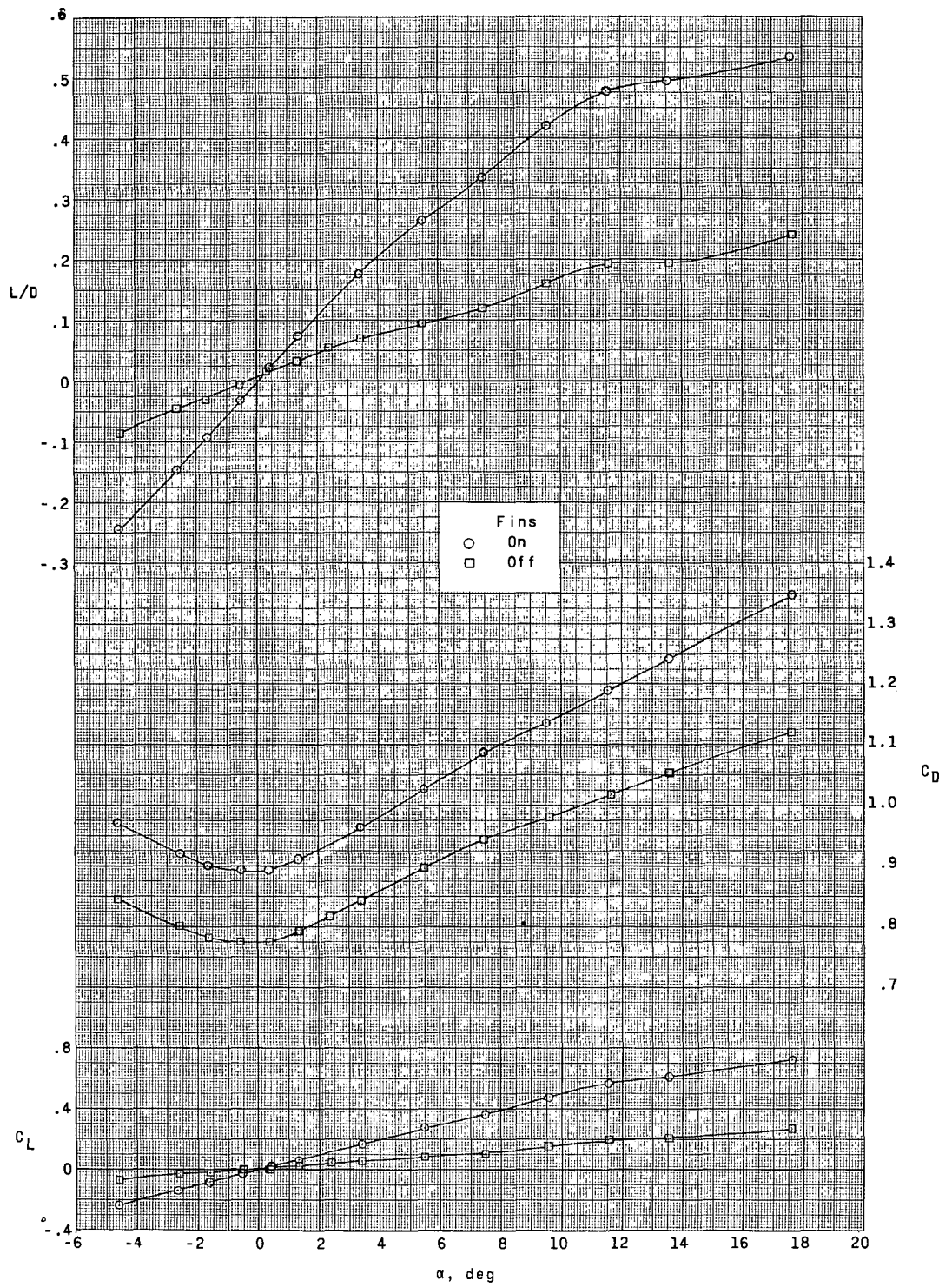
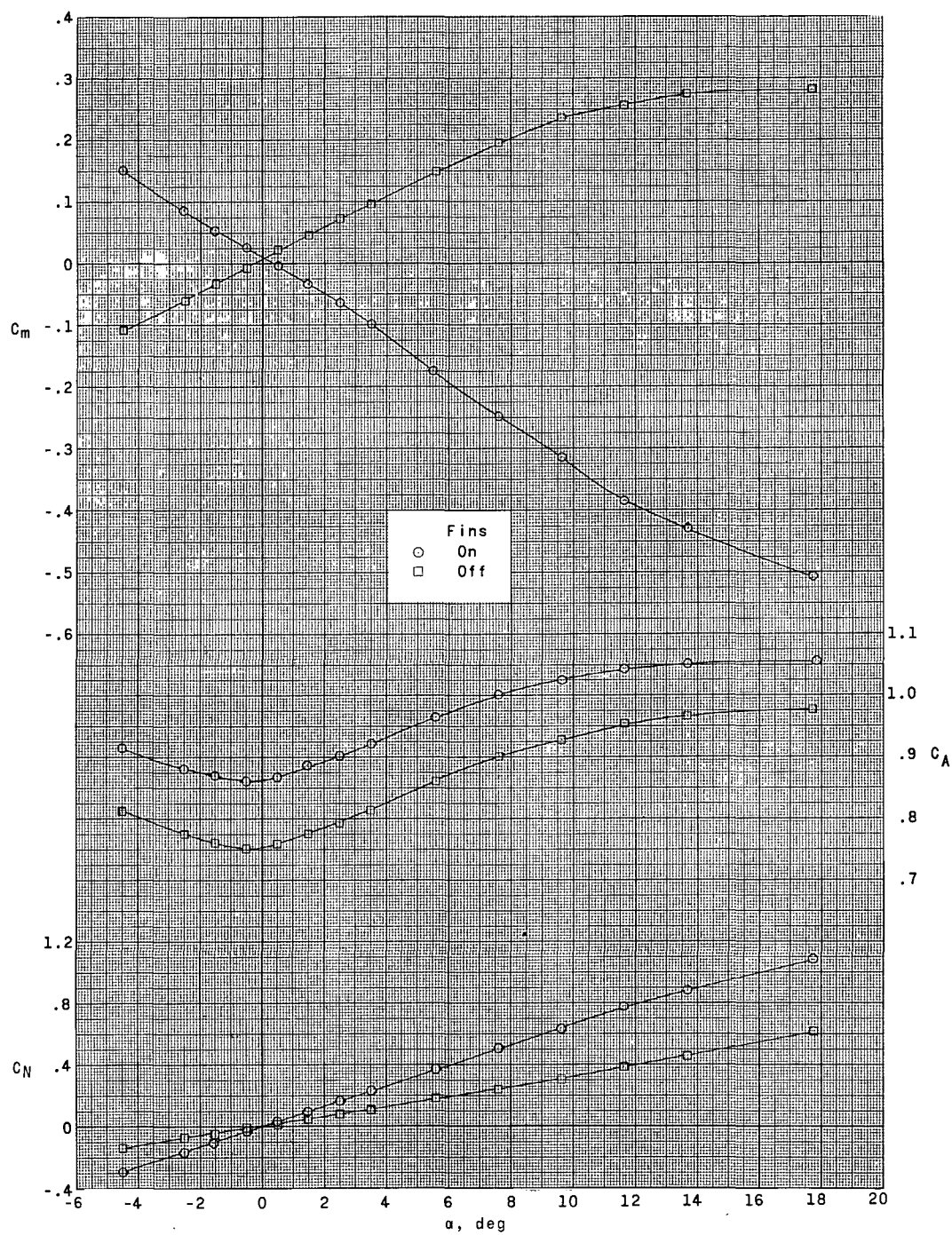
(a) $M = 1.50$.

Figure 6.- Longitudinal aerodynamic characteristics of model.



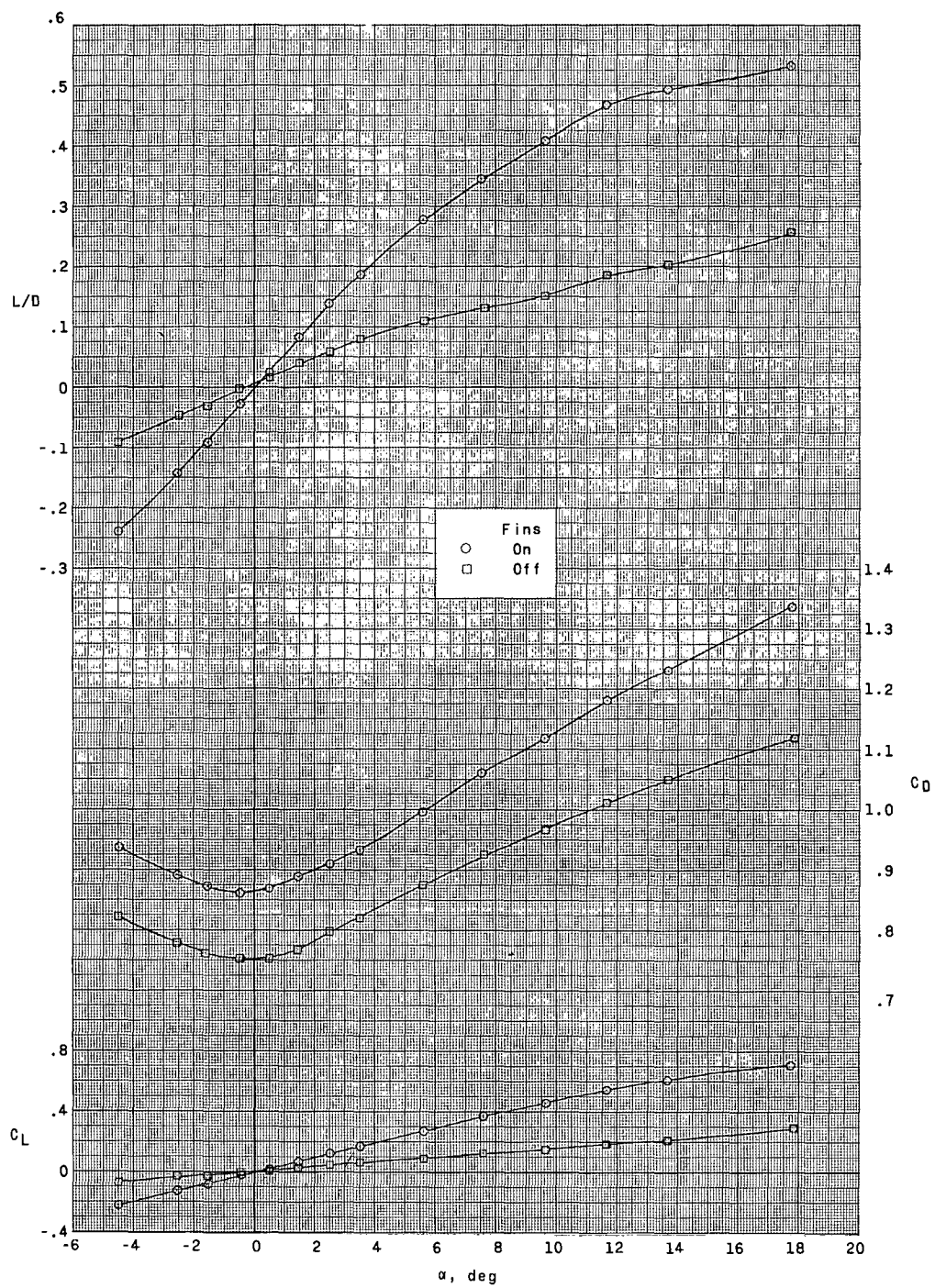
(a) Concluded.

Figure 6.- Continued.



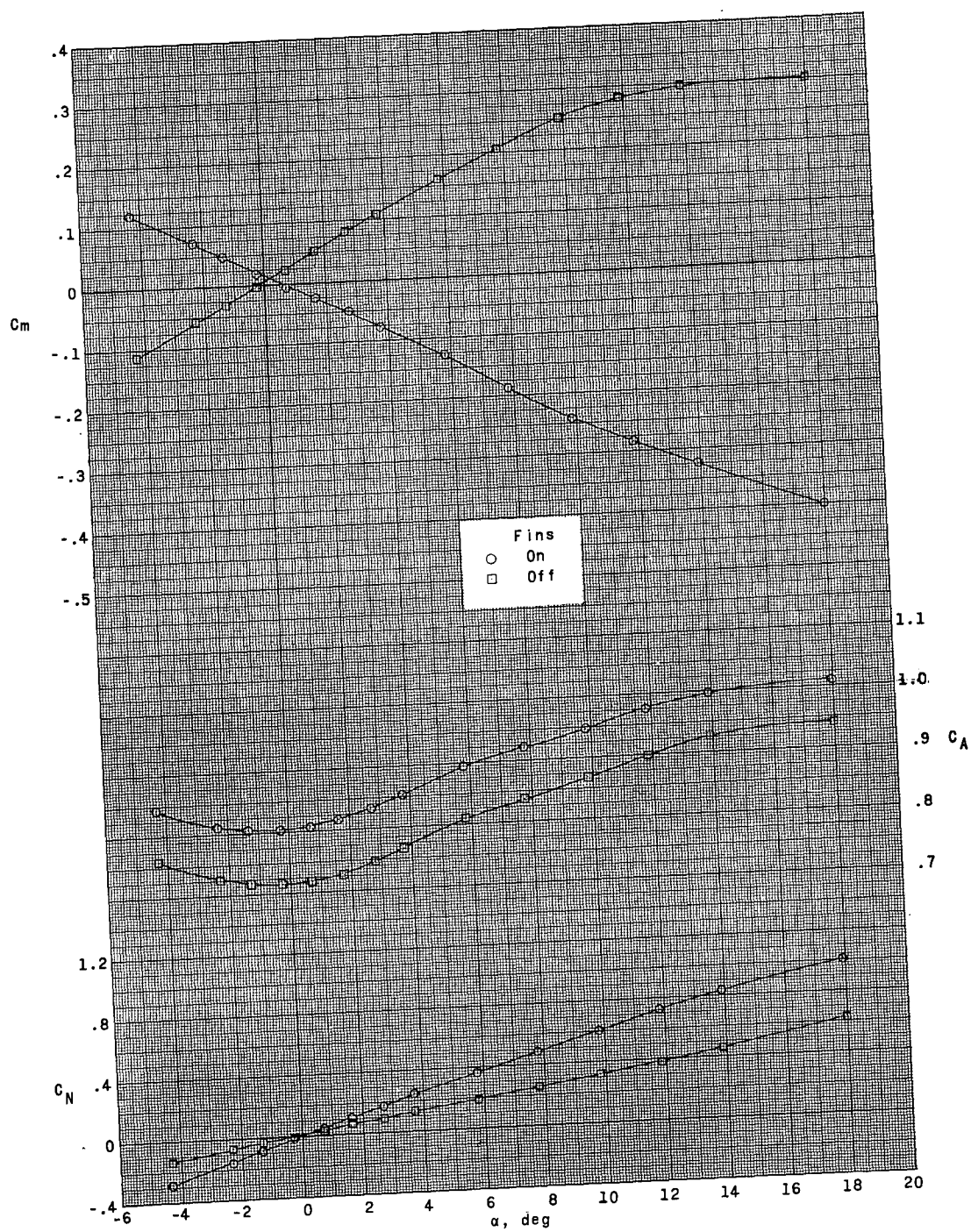
(b) $M = 1.57$.

Figure 6.- Continued.



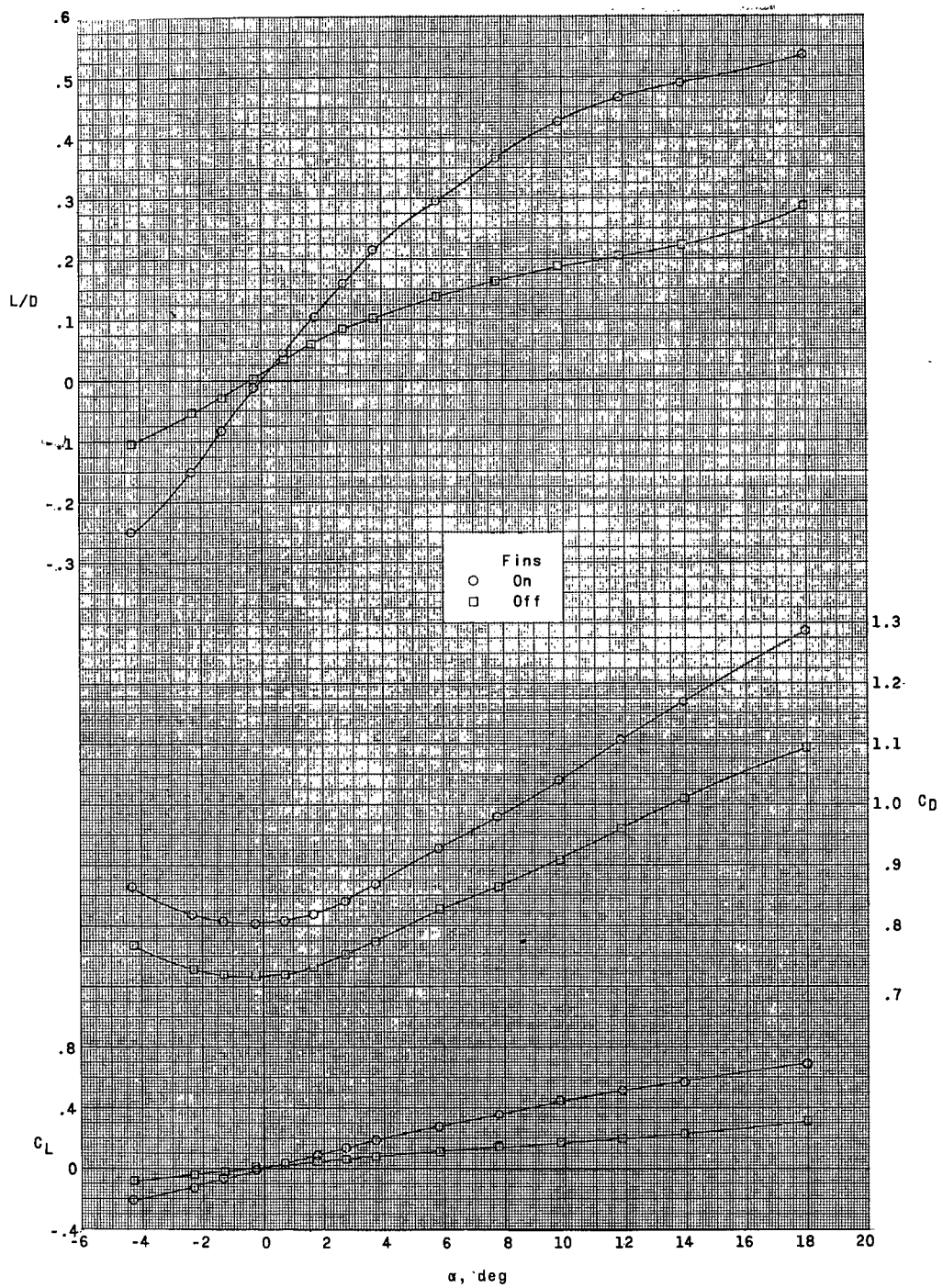
(b) Concluded.

Figure 6.- Continued.



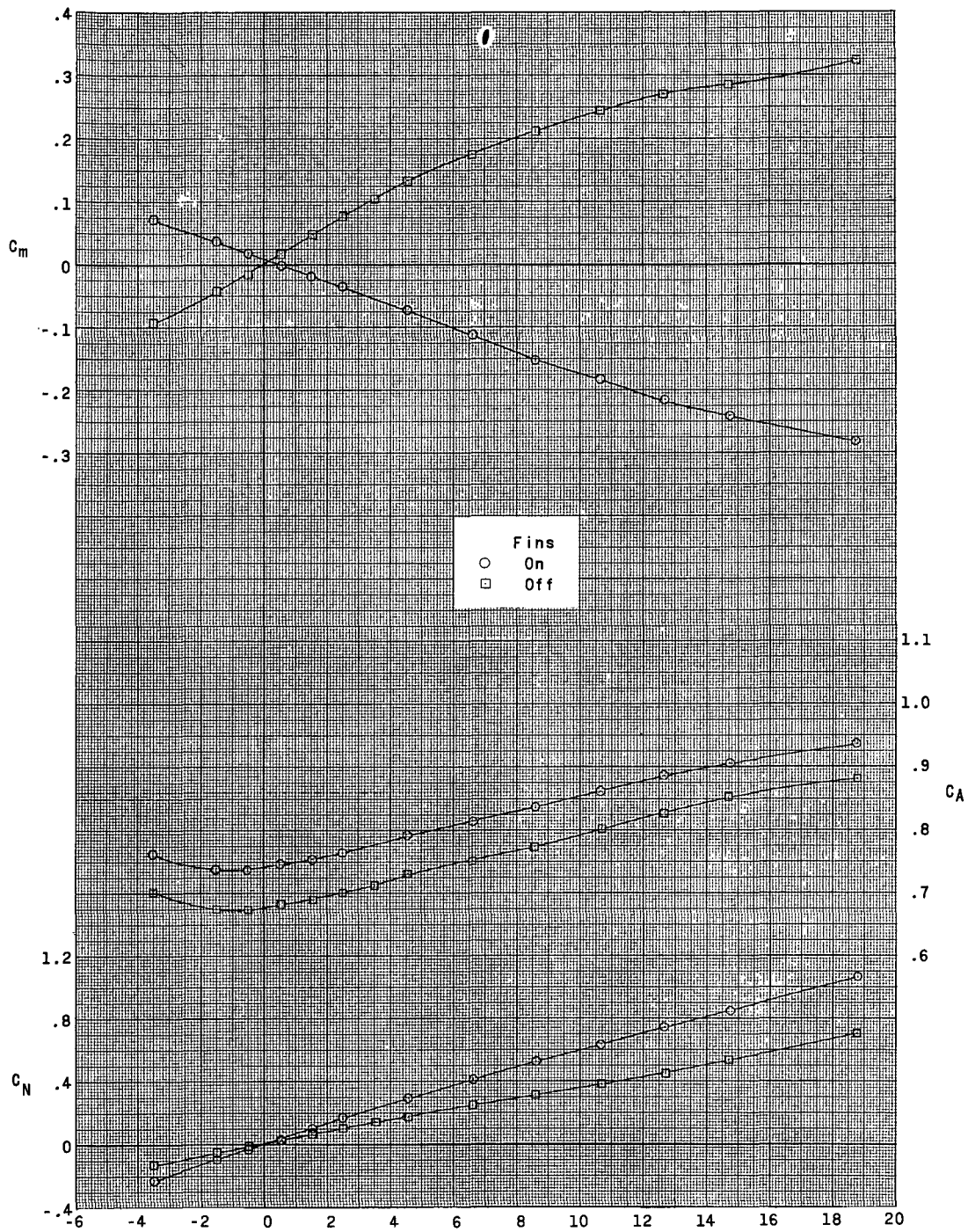
(c) $M = 1.80$.

Figure 6.- Continued.



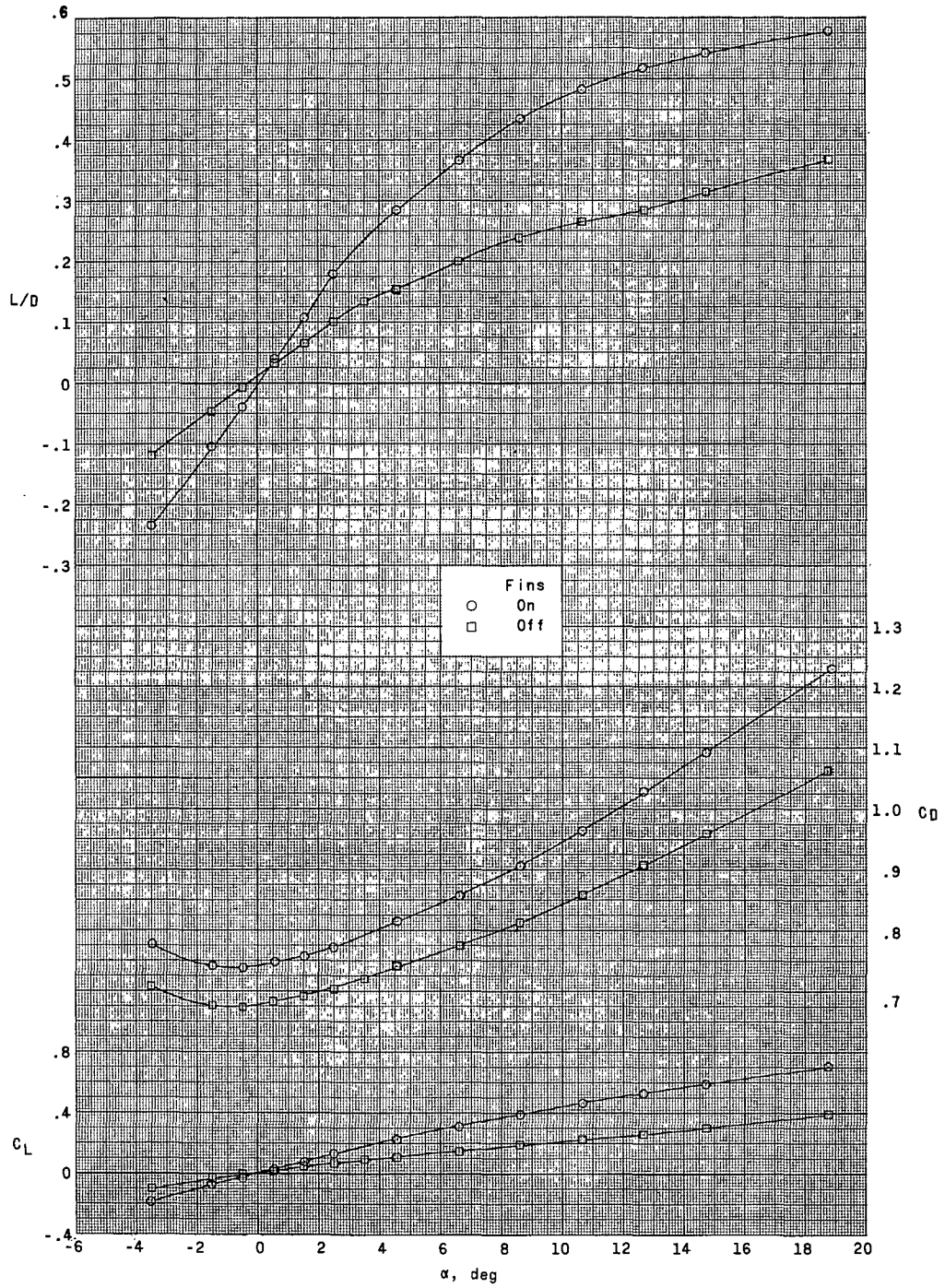
(c) Concluded.

Figure 6.- Continued.



(d) $M = 2.16$.

Figure 6.- Continued.



(d) Concluded.

Figure 6.- Concluded.

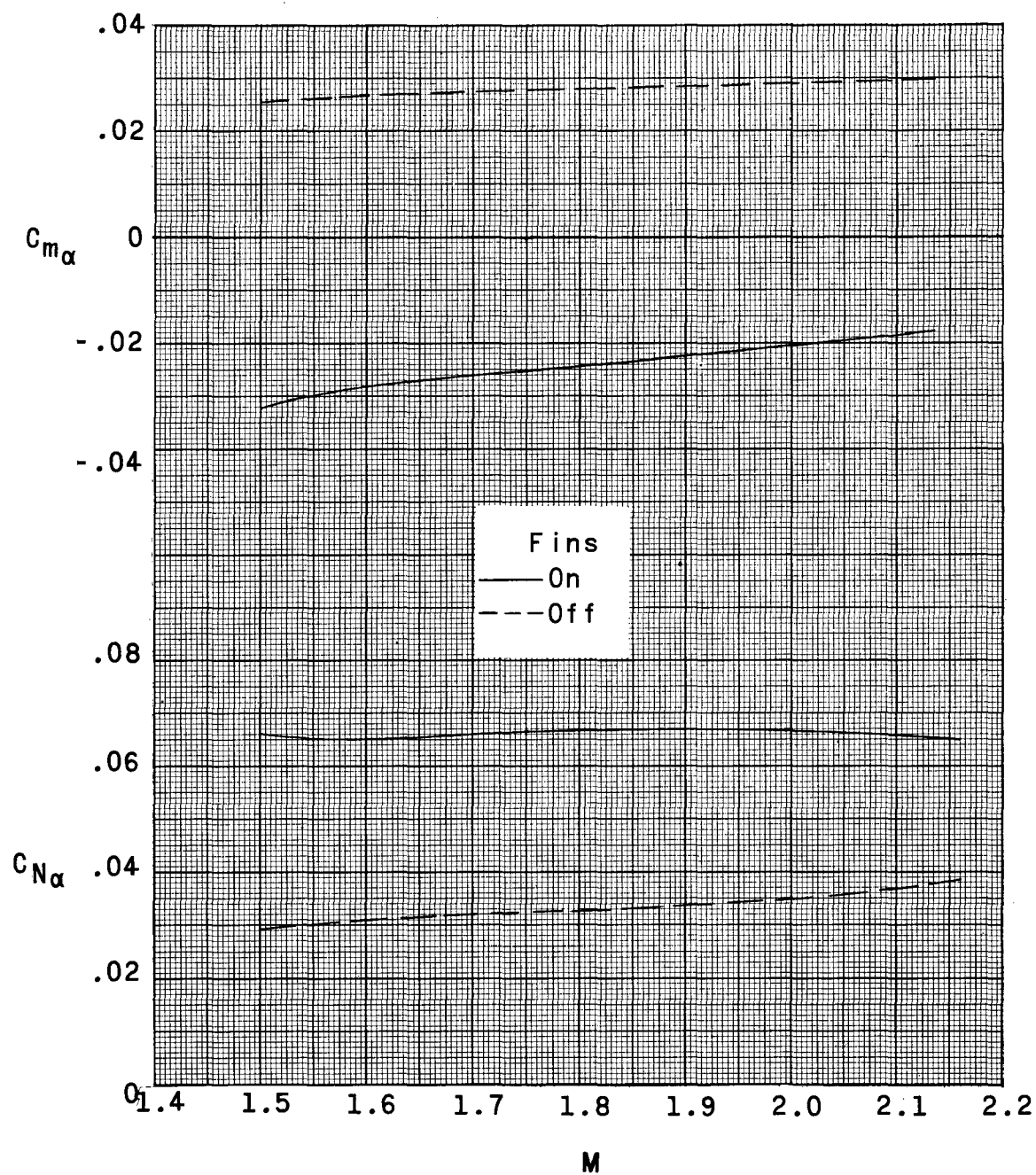


Figure 7.- Summary of longitudinal aerodynamic characteristics of model.

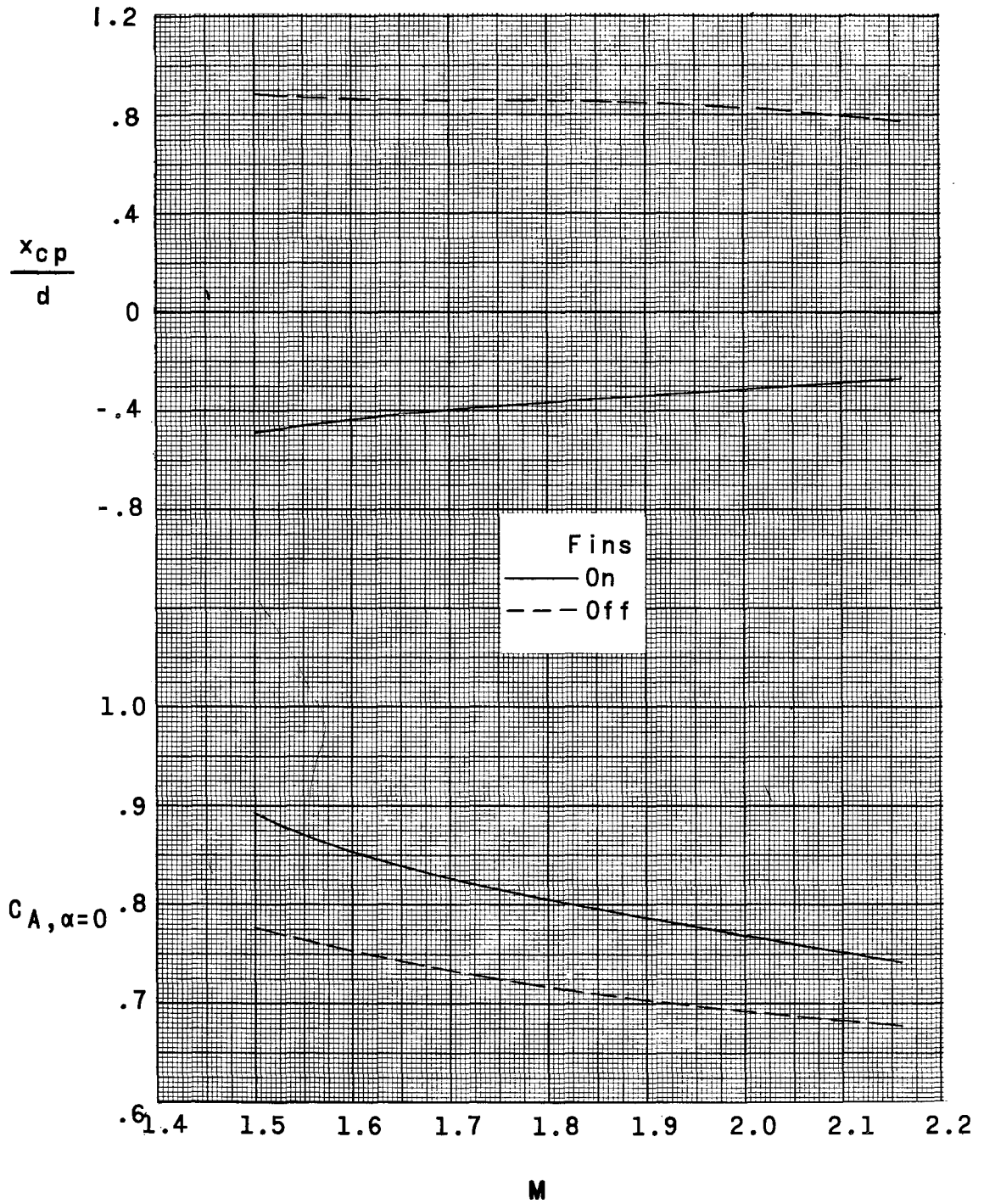


Figure 7.- Concluded.